International Journal of Nanomedicine

Dovepress
open access to scientific and medical research

Open Access Full Text Article

ORIGINAL RESEARCH

Green synthesis of AgNPs@PPE and its *Pseudomonas aeruginosa* biofilm formation activity compared to pomegranate peel extract

This article was published in the following Dove Press journal:
International Journal of Nanomedicine

Reza Habibipour[1]
Leila Moradi-Haghgou[1]
Abbas Farmany[2]

[1]Department of Microbiology, Hamedan Branch, Islamic Azad University, Hamedan, Iran; [2]Dental Research Center, School of Dentistry, Hamadan University of Medical Sciences, Hamadan, Iran

Background: Bacteria are able to form biofilm on the biotic and abiotic surfaces which helps to protect themselves from deleterious conditions, predation, desiccation, and exposure to antibacterial substances. About 80% of bacterial infections are caused by those bacteria living in the biofilm. *Pseudomonas aeruginosa*, a gram-negative, non-fermentative bacillus, and the ubiquitous bacterium is an important opportunistic pathogen notorious for biofilm formation and is remarkably resistant against most antibiotics multiple front-line antibiotics, which significantly contributes to eradication failure. The aim of this paper was to evaluate the anti-biofilm formation activity of Ag@PPEs gainst *P. aeruginosa* bacteria.

Methods: An aqueous extract of black pomegranate peel was used for the synthesis of silver nanoparticles (AgNPs@PPE). The characteristics, anti-biofilm formation and cell toxicity of AgNPs@PPE were examined in vitro.

Results: Absorbance at λ_{max} 372 nm which is related to the surface plasmon resonance, confirms the AgNPs@PPE formation. XRD pattern showed the face-centered qubic (fcc) crystalline structure of AgNPs. TEM images showed that spherical AgNPs size is ranged between 32 and 85 nm. The AgNPs@PPE showed inhibition effect against *P. aeruginosa* biofilm formation at 0.1 to 0.5 mg/ml concentrations. Cell toxicity assay showed that at 400 µg/ml, AgNPs@PPE were safe without a significant toxicity in L929 cell line.

Conclusion: These data indicate that co-treatment of PPE and AgNPs@PPE significantly decreased the biofilm formation rate. Furthermore, no significant toxicity of AgNPs@PPE was shown against L929 cell line at 400 µg/ml concentration.

Keywords: AgNPs, green synthesis, pomegranate peel extract, antibacterial activity

Introduction

Nowadays it has been proved that bacteria are able to form cellular assemblies on the biotic and abiotic surfaces, embedded in the matrix of extracellular polymeric compounds as a biofilm.[1,2] This biofilm helps microbial communities to protect themselves from deleterious conditions, predation, desiccation, and exposure to antibacterial substances, improved acquisition of nutrients and also as an important factor in the disease cycle of bacterial pathogens.[3–6] It has been reported that about 80% of the bacterial infections are caused by those bacteria living in the biofilm.[7]

Pseudomonas aeruginosa, a gram-negative, non-fermentative bacillus, and the ubiquitous bacterium, is an important opportunistic pathogen notorious for biofilm formation.[6,8] *P. aeruginosa* is remarkably resistant against most antibiotics multiple front-line antibiotics, which significantly contributes to eradication failure.[9]

Correspondence: Reza Habibipour
Department of Microbiology, Islamic Azad University, Hamedan Branch, Prof. Mousivand Blvd., Imam Khomeini Blvd, Hamedan 6518115743, Iran
Email habibipour@iauh.ac.ir

Abbas Farmany
Dental Research Center, School of Dentistry, Hamadan University of Medical Sciences, Shahid Fahmideh Street, Hamadan 6517838677, Iran
Email a.farmany@usa.com

submit your manuscript | www.dovepress.com
DovePress
http://doi.org/10.2147/IJN.S209912

Pomegranate (*Punica granatum L. Punicaceae*) is a native fruit in China, Iran, Afghanistan, and Indian subcontinent.[10] Due to the high content of phenolic compounds, since ancient times, this fruit has been used to treat several diseases as a traditional medicinal source which can treat many infectious diseases.[11,12] The antibacterial activity of pomegranate has been reported extensively in several bacteria such as *Escherichia coli, Staphylococcus aureus, Vibrio cholera, Bacillus subtilis, Bacillus cereus, Bacillus coagulans, Shigella dysentriae, Enterobacter cloacae, Pseudomonas fluorescens, Proteus vulgaris, Alcaligenes faecalis, Serratia marcescens, Arthrobacter globiformis, Micrococcus roseus, Micrococcus luteus, Mycobacterium phlei, Mycobacterium rodochrus*, and *Mycobacterium smegmatis*.[13–16]

Silver nanoparticles (AgNPs), in the form of colloidal particles, are one of the oldest common and famous antimicrobials.[17,18] The general approaches for the synthesis of AgNPs are chemical, physical, and biological.[19] Main conventional physical methods are pyrolysis and spark discharge.[20] Chemical routes of AgNPs synthesis are based on the chemical reduction of silver ion using reducing/stabilizing agents such as borohydride, thio-glycerol, and 2-mercapto-ethanol which are toxic and hazardous.[20] Biological methods including fungi, bacteria, and plant extracts.[21–30] Chemical and physical synthesis methods of AgNPs may trigger toxicity for human being and other creature's cells. Therefore establishing green synthesis of AgNPs is highly recommended to reduce the toxic effects. Using the plant extracts as reducing and stabilizing agents not only decrease the toxic effects of AgNPs, but also, in some plant extracts such as pomegranate extract, increase its antibacterial effects.[31] Pomegranate extract contains some polysaccharides, polyphenols, flavonoids (specially, flavonols, flavones, and flavanones), and anthocyanidins with high antioxidant activity.[31,32] It is interesting that pomegranate extract-based nanoparticles show a high colloidal stability.[32] At this time, the antibacterial activity of pomegranate extract-based AgNPs against *E. coli* was considered without investigating anti-biofilm formation activity evaluation. Herein, we aimed to evaluate the anti-biofilm formation activity potential of Ag@PPE and pomegranate peel extract (PPE) against gram-negative *P. aeruginosa* bacteria was investigated.

Materials and methods

All chemicals used in this study were purchased from Sigma.

Preparation of the PPE

Black peel pomegranate fruit was collected from a local pomegranate garden (Saveh, Iran). Pomegranate rinds were dried at 50°C in an oven, and then powdered. The powder (50 g/L) was mixed with 200 mL of 70% ethanol and agitated using a rotary shaker (150 rpm) for 24 hrs and filtered. The residue was re-extracted with 200 mLof fresh solvent, filtered and the extract was pooled. Following that, the solvent was evaporated by a rotary (Heidolph, model LABOROTA Digital 4003 equipped with Rotavac sensor pump, Germany) at 40°C. It was boiled in a 50 mL of deionized water and allowed to cool. Finally, the cooled extract was filtered and stored in a refrigerator at 4°C. The resulting extract was used as PPE solution.

Preparation of AgNPs@PPE

The AgNPS@PPE was biosynthesized in a one-step process.[33] Briefly, PPE solution was added drop-by-drop to an aqueous solution of $AgNO_3$ till the solution colored to light-yellow. The color change of the solution from yellow to brownish-yellow indicates the success biosynthesis process of AgNPs@PPE.

Bacteria and culture conditions

Gram-negative *P. aeruginosa* bacteria (ATCC: 10662) used in this study. The organism was sub-cultured in nutrient agar media at 37°C and incubated overnight.

Biofilm production assay

Microtiter dish biofilm formation assay was used to evaluate the bacterial biofilm formation.[34] Briefly, 180 µL of TSB was spread into a sterile 96-well flat-bottomed microtiter plate (Orange). To this, 100 µL of the prepared PPE and AgNPs@PPE solutions was added. Then, 20 µL of bacteria suspension (overnight culture in TSB, equal to 0.5 McFarland) was added to wells (except negative control wells) and the plates were incubated at 37°C for 6, 12, 18, and 24 hrs. After incubation, the content of the wells was decanted into a waste container and each well was washed three times with 200 µL of phosphate buffer to remove non-adherent cells and dried. Staining the adhered cells was made by adding 220 µL of crystal violet (0.1%). To quantify the adhered cells, 220 µL of glacial acetic acid (33% v/v) was added to wells for 15 mins. The absorption of the eluted stain was read out using a microtiter plate reader at 630 nm (Universal microplate reader ELX 800; Bio-tek instruments Inc., Winooski, USA). Based on the

measured ODs, treatments were classified into four categories as: strong (OD >4x ODc), moderate (OD >2x ODc, but ≤4x ODc), weak (OD > ODc, but ≤2x ODc), and non-biofilm forming (OD ≤ ODc). The cut-off OD (ODc) was defined as equivalent to three times standard deviation above the mean OD of the negative control. All tests were made in triplicates and the data were averaged.[35]

Kinetics of biofilm formation

Aliquot of an overnight culture of *P. aeruginosa* was transferred into a sterile microplate to evaluate the biofilm formation kinetics in the presence of different concentrations of AgNPs@PPE, PPE, and both of them. The plates were incubated at 37 ºC for 24 hrs. At different times (every 6 hrs) the biofilm formation was detected.[36]

Inhibition of biofilm formation

The OD (630 nm) of samples was used to calculate the inhibition percentage as,[37]

$$inhibition\% = \frac{ODincontrol - ODintreatment}{ODincontrol} \times 100$$

Cell toxicity assay of PPE and AgNPs-PPE

To test the potential toxicity of AgNPs-PPE and PPE against a cell line, a fibroblastic cell line (L 929 cell line) was cultured in RPMI containing 10% fetal bovine serum with 50 IU/mL penicillin and 50 µg/mL streptomycin in a 5% CO_2 atmosphere at 37°C. The cultured cells were treated with different concentrations of PPE and AgNPs-PPE (100, 200, 300, 400, and 500 µg/mL). MTT assay was applied to test the cell viability. Briefly, the cells were cultured in a 96-well plate and incubated for 3 hrs with MTT solution. 200 µL DMSO was added to each well to solubilize formazan particles, and finally, the absorbance was read at 580 nm by an ELISA reader (Microplate reader labsystem multiscan).

Statistical analysis

Analysis of variance of the obtained data was performed using the SAS statistical package (SAS Institute Inc., Cary, NC, USA). Data were transformed to arcsine square root values to normalize variances prior to analysis. Treatment means were separated using the Waller Duncan k ratio *t*-test at $P<0.05$.

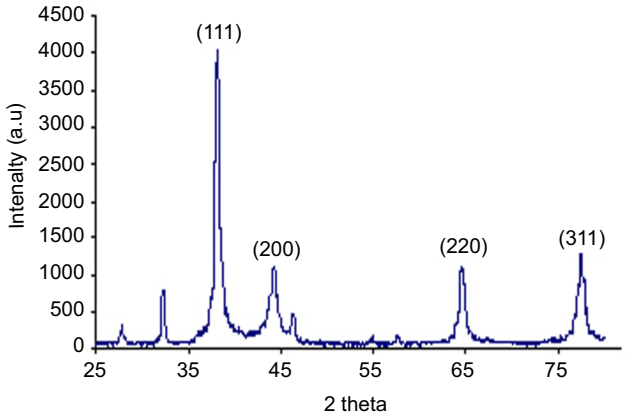

Figure 1 XRD pattern of AgNPs@PPE.
Abbreviation: XRD, X-ray diffraction.

Results

AgNPs@PPE characteristics

X-ray diffraction (XRD) pattern of AgNPs@PPE

XRD pattern of synthesized nanoparticles is shown in Figure 1. Main peaks registered at 2θ of 32.28, 38.18, 44.53, 64.68, and 77.58 are indexed as the diffraction of (111), (200), (220), and (311), respectively.

Ultraviolet-vis spectrophotometry (UV-vis) spectra of AgNPs@PPE

The UV-vis absorption spectra of AgNPs@PPE are shown in Figure 2. Main absorption peak at 372 nm is related to the characteristics of surface plasmon resonance (SPR) absorption.

Photoluminescence (PL) spectra of AgNPs@PPE

A PL spectrum of AgNPs@PPE was registered for 380 nm excitation wavelength. As shown in Figure 2, AgNPs@PPE has an intense emission at 420 nm.

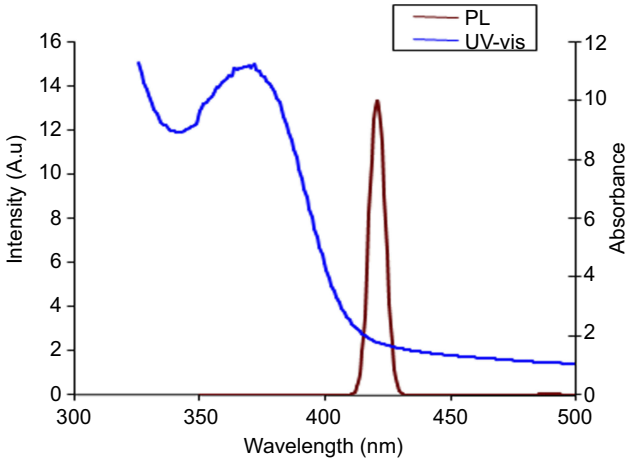

Figure 2 UV-vis and PL spectra of AgNPs@PPE.
Abbreviations: PL, photoluminescence; UV-vis, ultraviolet-vis spectrophotometry.

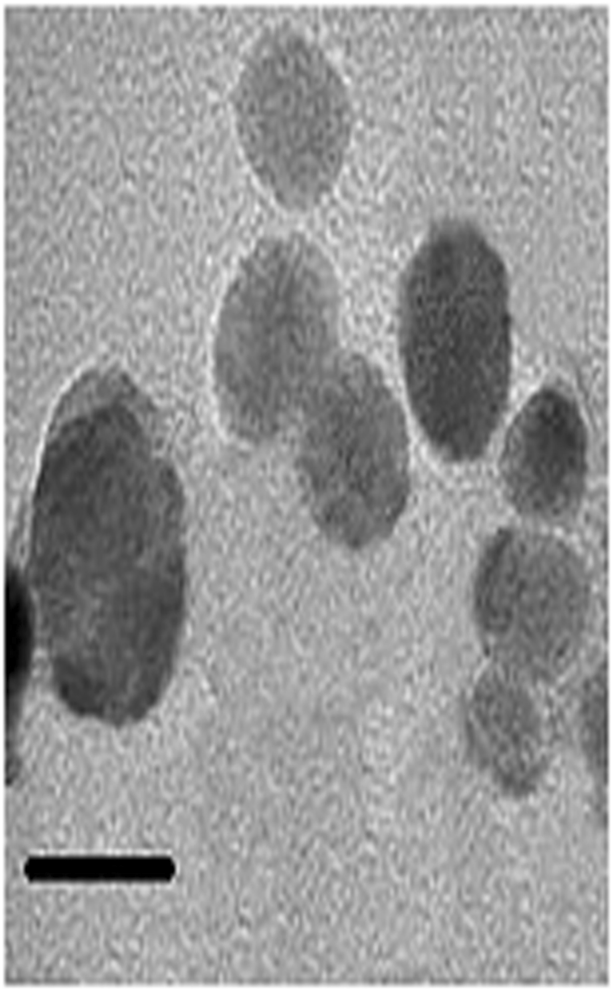

Figure 3 TEM image of the AgNPs@PPE (scale bar is 50 nm).
Abbreviation: TEM, transmission electron microscopy.

TEM of AgNPs@PPE

Figure 3, displays the TEM image of AgNPs. According to the TEM image, during the synthesis process, colloidal AgNPs with diameter ranged between 32 and 85 nm were obtained.

Biofilm formation assay and kinetics of biofilm formation

The results of biofilm formation kinetics in the PPEs and AgNPs@PPE treatments at different times are presented in Figure 4. As shown in Figure 4A, only in the 0.05 and 0.3 mg/mL AgNPs@PPE treatments, the bacterial biofilm was formed (strong category) while in the other treatments no such biofilm was formed (weak or non-biofilm category).

Based on the results of this study, a strong biofilm was formed after 12, 18, and 24 hrs incubation which can be classified as strong, though there was not formed a bacterial biofilm after 6 hrs incubation (non-biofilm category). It seems that 6 hrs incubation is the growth phase of bacterial biofilm formation. At this point, the kinetics of biofilm formation in the AgNPs@PPE and PPE treatments were similar. Also, strong biofilm formation was observed after 18 hrs of incubation which was decreased at 24 hrs (Figure 4B and C).

As shown in Figure 4B and C, at 12 hrs incubation with 1.0 and 5.0 mg/mL PPE, strong biofilm was formed while it was decreased at other treatments. Also, after 18 hrs incubation with PPE, a strong biofilm was formed only at 1.0 mg/mL, while in other treatments, a weak biofilm was formed. At 24 hrs incubation, strong and moderate biofilm forming were observed at 1.0 and 5.0 mg/mL PPE, respectively. However, weak biofilms were formed at 10.0 and 50.0 mg/mL of PPE treatments (Figure 4C).

The results of co-treatment experiments (Figure 4A) are given below:

The lowest anti-biofilm effect (strong biofilm formation) was observed at 0.05, 0.1, and 0.15 mg/mL AgNPs@PPE with 1.0 mg/mL PPE co-treatments.

In 0.05 mg/mL AgNPs@PPE with 1.0 mg/mL PPE treatment, the rate of biofilm formation was increased till 18 hrs, while it was decreased at 24 hrs. Similar results were obtained for co-treatments of 0.05 mg/mL AgNPs@PPE with 1.0, 5.0, 10.0 mg/mL PPE. However, at 50.0 mg/mL PPE, the kinetics was linear which shows an inhibition effect on the biofilm formation.

In 0.1 mg/mL AgNPs@PPE treatment with PPE, the biofilm formation kinetics was decreased in the presence of 10.0 and 50.0 mg/mL PPE. The biofilm formation kinetics of 0.1 mg/mL AgNPs@PPE and 5.0 mg/mL PPE treatment was similar to 0.05 mg/mL AgNPs@PPE and 5.0 mg/mL PPE.

In 0.15 mg/mL of AgNPs@PPE treatment with different concentrations of PPE, only at 24 h and 50.0 mg/mL PPE, a low biofilm-forming characteristics was obtained.

The results of 0.2 mg/mL AgNPs@PPE treatment with different concentrations of PPE showed that at 1.0 mg/mL PPE, after 15 hrs, no any inhibition effects on the biofilm formation were seen, though, in other co-treatments, bacterial biofilm formation kinetics was decreased.

The results of 0.3 mg/mL AgNPs@PPE treatment with different concentrations of PPE showed that except than 0.3 mg/mL AgNPs@PPE with 5.0 mg/mL of PPE, in other treatments, the growth rate was exponential with similar kinetics trend.

At 0.4 and 0.5 mg/mL AgNPs@PPE treatments with PPE, no any *P. aeruginosa* biofilm was formed (non-biofilm category).

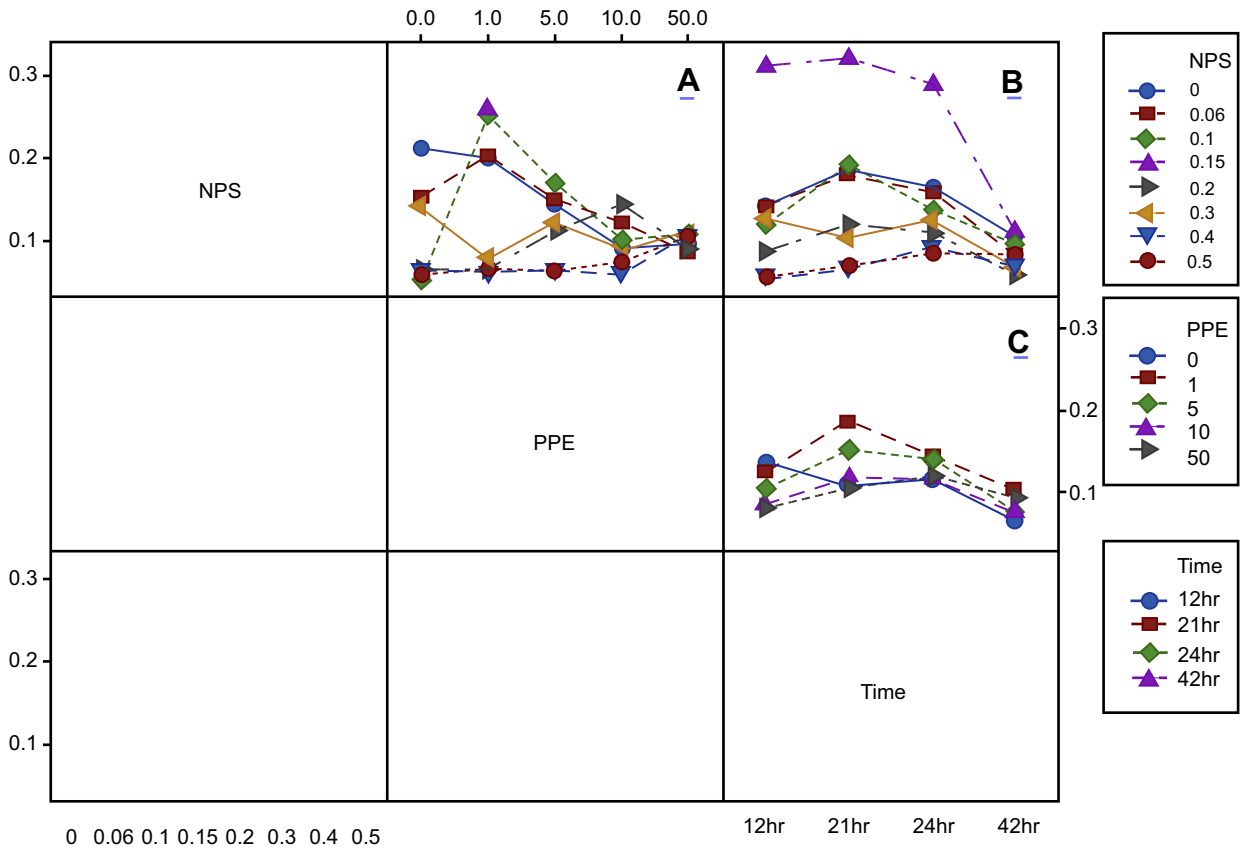

Figure 4 Kinetic of biofilm formation by *Psuedamonas aeruginosa* at different treatments: (**A**) AgNPs@PPE and PPE co-treatment; (**B**) AgNPs@PPE treatment at 6, 12, 18, 24 hrs; (**C**) PPE treatment at 6, 12, 18, 24 hrs.

As a result of Figure 4B, in the most co-treatment experiments, at 12 hrs incubation, the biofilm formation rates were low which could be related to the bacterial growth phase kinetics and after 18 hrs incubation, highest biofilm formation was seen. It is interesting that in each timeline, at different concentrations of AgNPs@PPE, the biofilm formation trends were similar.

Inhibition of biofilm formation

The results of the inhibition effect of AgNPs@PPE and PPEs on the bacterial biofilm formation are presented in Tables 1 and 2.

As shown in Table 1, higher biofilm formation rates were obtained at 18 hrs incubation. At this incubation time, for 0.1–0.5 mg/mL AgNPs@PPE, the inhibition in the biofilm formation was significantly increased. Similar results were obtained for PPE.

Cell toxicity

Cell viability assay was used to test the potential toxicity of synthesized nanoparticles. As shown in Figure 5, AgNPs-PPE in the concentration of 400 and 500 µg/mL significantly decreased cell viability, however when the PPE alone was treated the toxicity of particles remarkably decreased., where in the concentration of 400 µg/mL the particles were safe without significant toxicity. Although the cell viability of PPE in the concentration of 500 µg/mL was higher than AgNP-PPE, 63±4.1% compared to 57 ±3.9%, this concentration shows toxic effect. The results for 500 µg/mL were same for both treatments, as cell viability was significantly decreased in both treatments.

Discussion

In this study, PPE was used to develop a green process of AgNPs synthesis. To confirm the AgNPs@PPE formation and obtain its structural information, X-ray diffraction pattern of nanoparticles was obtained (Figure 1). Peaks at 32.28, 38.18, 44.53, 64.68, and 77.58 (2θ) are indexed as (111), (200), (220), and (311) diffractions, respectively. Comparing the obtained reflection peak positions resemble the standard diffraction pattern (JCPDS#89-3722), which possess the face-centered cubic (fcc) crystalline structure.

Table 1 Biofilm inhibition (%) of *Pseudamonas aeruginosa* with AgNPs@PPE and PPE treatments

Treatment (mg/mL)	6 hrs	±SD	12 hrs	±SD	18 hrs	±SD	24 hrs	±SD
Ag NP (0.05)	15.5	±0.1	87.2	±0.0	65.6	±0.3	70.9	±0.1
Ag NP (0.1)	16.2	±0.1	6.3	±0.0	244.5	±0.2	0.2	±0.1
Ag NP (0.15)	14.9	±0.0	6.0	±0.1	235.0	±0.6	2.9	±0.2
Ag NP (0.2)	19.7	±0.6	13.0	±0.8	221.1	±0.2	8.4	±0.6
Ag NP (0.25)	24.6	±0.8	10.6	±0.8	227.0	±0.8	11.4	±0.4
Ag NP (0.3)	24.5	±0.1	11.2	±0.2	232.1	±0.6	15.4	±0.6
Ag NP (0.35)	24.6	±0.1	5.7	±0.0	225.5	±0.3	21.8	±0.6
Ag NP (0.4)	33.1	±0.1	5.2	±0.1	233.5	±0.3	22.8	±0.4
Ag NP (0.45)	38.3	±0.0	5.1	±0.6	235.7	±0.8	7.4	±0.1
Ag NP (0.5)	48.7	±0.6	1.2	±0.1	243.8	±0.8	10.4	±0.1
PPE (1)	61.0	±0.4	89.0	±0.3	65.6	±0.3	79.6	±0.2
PPE (5)	65.5	±0.1	70.8	±0.7	244.5	±0.6	58.7	±0.2
PPE (10)	72.0	±0.1	28.2	±0.0	235.0	±0.0	19.1	±0.3
PPE (50)	154.5	±0.4	33.4	±0.7	221.1	±0.1	33.3	±0.1

Appearance of two unpredicted diffraction peaks at 2θ of 32.38 and 46.43 may be related to the presence of organic (phytochemical) compounds in the PPE. The presence of unassigned crystalline peaks at 32.38 and 46.43 was also reported in the literature.[38,39] UV-vis absorption spectra at 372 nm are related to the mutual vibration of SPR free electrons at the AgNPs@PPE structure.

To evaluate the PL photo-activity, the colloidal AgNPs@PPE was photo-excited at 380 nm and its emission peaks were registered. A characteristic PL peak was recorded at 420 nm which is in agreement with other reports.[40] Also, TEM images of AgNPs@PPE clearly show the formation of spherical nanoparticles with a size of 32–85 nm.

Colloidal AgNP is one of the most common antimicrobial materials.[17,18] Antibacterial properties of this nanomaterial against yeast, *E. coli, S. aureus, B. megaterium, P. vulgaris*, and *S. sonnei* were examined and a lot of studies have reported that AgNPs can inhibit the formation of life-threatening biofilms. In this study, we have tested the ethanolic extracts of PPEs in different concentrations for anti-biofilm activity against *P. aeruginosa* separately or in co-treatment with AgNPs@PPE.

In this study, the concentration of 10.0 mg/mL PPE showed antibacterial activity which is in agreement with Raju et al, results that showed an aqueous and alcoholic extract of pomegranate has a maximum antibacterial activity. In this regard, ethanolic extract of black pomegranate peel was able to inhibit not only the growth of *P. aeruginosa* but also the biofilm formation which is similar to the results obtained for *S. aureus*.[15]

The most active constituents in the pomegranate extract are phytochemical such as gallotannins, ellagic acid derivatives, catechins and procyanidins, punicalagin, castalagin, granatin, catechin, gallocatechin, kaempferol, quercetin, and flavonols.[32] Antimicrobial activities of phenolic compounds may possess multiple modes of action. The main mechanism for phenolic toxicity against microorganisms is its reaction with sulfhydryl groups of membrane proteins and inhibition of enzymes such as glycosyltransferase resulted in the microbial cell lysis.[12,41,42] Phenolic compounds can also bind to substrates such as minerals, vitamins, and carbohydrates making them unavailable for microorganisms.[43] *P. aeruginosa* as gram-negative bacteria has an outer membrane which serves as a selective permeability barrier, protecting bacteria from harmful agents such as detergents, drugs, toxins, degradative enzymes, and penetrating nutrients to sustain bacterial growth. *P. aeruginosa* is able to adhere and form the biofilm on the surfaces, causing severe resistance against many antibiotics and disinfectants which leads to the battle of sanitizing.[44] In this study, we have found that AgNPs@PPE and PPE could inhibit the *P. aeruginosa* biofilm formation. However, at low AgNPs@PPE concentrations, there might be a resistance to AgNPs@PPE.[45] AgNPs uptake has a concentration-dependent pattern.[17] Despite its evident anti-biofilm activity, all treatments containing AgNPs@PPE did not prevent biofilm formation under the experimental conditions of this study. Mode of action of AgNPs@PPE to bacterial communities is still unknown. Disruption of cellular membrane or membrane potential, genotoxicity, oxidation of proteins, interruption of energy transduction, and the formation of ROS and release of toxic

Table 2 Biofilm inhibition (%) of *Pseudamonas aeruginosa* with AgNPs@PPE and PPE co-treatments

Co-treatment (mg/mL)	6 hrs	±SD	12 hrs	±SD	18 hrs	±SD	24 hrs	±SD
Ag NP 0.05 - PPE 1	70.1	±0.1	98.1	±0.5	95.6	±0.5	68.4	±0.7
Ag NP 0.05 - PPE 5	5.6	±0.1	48.3	±0.1	49.6	±0.1	72.8	±0.1
Ag NP 0.05 - PPE 10	42.8	±0.9	46.2	±0.3	89.0	±0.3	41.7	±0.6
Ag NP 0.05 - PPE 50	150.6	±0.8	35.5	±0.0	187.5	±0.0	12.1	±0.1
Ag NP 0.1 - PPE 1	82.4	±0.1	122.1	±0.9	343.8	±0.1	61.6	±0.1
Ag NP 0.1 - PPE 5	74.6	±0.1	58.9	±0.8	10.2	±0.9	88.0	±0.7
Ag NP 0.1 - PPE 10	51.9	±0.9	36.7	±0.0	189.8	±0.1	34.0	±0.2
Ag NP 0.1 - PPE 50	103.9	±0.8	18.5	±0.1	87.5	±0.8	33.5	±0.2
Ag NP 0.15 - PPE 1	64.9	±0.1	133.1	±0.1	219.7	±0.1	10.6	±0.5
Ag NP 0.15 - PPE 5	36.3	±0.1	61.0	±0.0	73.0	±0.0	34.0	±0.1
Ag NP 0.15 - PPE 10	47.4	±0.7	42.2	±0.1	63.5	±0.1	31.0	±0.1
Ag NP 0.15 - PPE 50	22.0	±0.7	16.1	±0.6	181.7	±0.2	22.8	±0.0
Ag NP 0.25 - PPE 1	25.9	±0.7	3.3	±0.4	238.6	±0.2	37.5	±0.9
Ag NP 0.25 - PPE 5	28.5	±0.6	46.8	±0.1	93.4	±0.1	34.0	±0.9
Ag NP 0.25 - PPE 10	57.7	±0.1	70.2	±0.1	10.9	±0.4	43.2	±0.1
Ag NP 0.25 - PPE 50	37.6	±0.6	19.7	±0.0	152.5	±0.0	26.1	±0.9
Ag NP 0.3 - PPE 1	29.2	±0.3	6.3	±0.2	221.1	±0.4	35.8	±0.1
Ag NP 0.3 - PPE 5	27.9	±0.1	37.0	±0.4	26.2	±0.3	35.5	±0.6
Ag NP 0.3 - PPE 10	90.2	±0.8	4.5	±0.2	165.6	±0.9	53.4	±0.7
Ag NP 0.3 - PPE 50	35.0	±0.6	27.3	±0.3	189.7	±0.3	47.0	±0.4
Ag NP 0.35 - PPE 1	22.7	±0.7	6.0	±0.1	212.4	±0.8	14.4	±0.4
Ag NP 0.35 - PPE 5	16.8	±0.4	13.6	±0.0	47.4	±0.0	44.2	±0.1
Ag NP 0.35 - PPE 10	61.0	±0.1	6.3	±0.6	115.3	±0.3	41.5	±0.5
Ag NP 0.35 - PPE 50	26.6	±0.3	20.3	±0.8	119.7	±0.5	33.5	±0.9
Ag NP 0.4 - PPE 1	22.7	±0.0	4.5	±0.0	232.8	±0.1	10.9	±0.0
Ag NP 0.4 - PPE 5	32.4	±0.2	8.5	±0.1	224.8	±0.1	16.4	±0.3
Ag NP 0.4 - PPE 10	88.3	±0.1	5.8	±0.2	225.5	±0.1	11.9	±0.2
Ag NP 0.4 - PPE 50	34.4	±0.5	27.0	±0.0	183.2	±0.1	48.5	±0.3
Ag NP 0.5 - PPE 1	38.3	±0.0	8.2	±0.0	222.6	±0.4	13.9	±0.0
Ag NP 0.5 - PPE 5	57.1	±0.2	6.9	±0.0	224.0	±0.8	11.6	±0.5
Ag NP 0.5 - PPE 10	101.3	±0.1	7.9	±0.0	224.0	±0.5	22.6	±0.4
Ag NP 0.5 - PPE 50	48.7	±0.5	22.1	±0.9	164.2	±0.4	32.5	±0.3

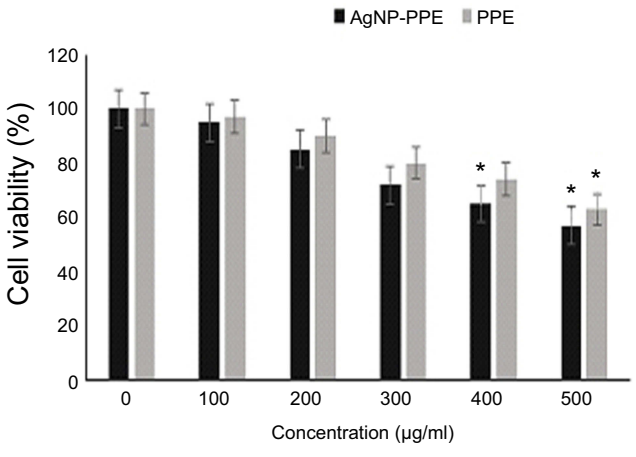

Figure 5 Cells viability of treatments with different concentrations of AgNPs-PPE and PPE after 48 hrs.

constituents are suggested as probable mechanisms of AgNPs@PPE anti-biofilm effects.[18]

Negatively charged AgNPs@PPE can be electrostatically repulsed from the negatively charged bacterial membranes. This may reduce their effective interactions.[46] Also, at ionic media; aggregation of AgNPs@PPE nanoparticles may reduce their effective penetration into the biofilm surfaces.[47]

The release of silver ions from AgNPs@PPE can penetrate the bacterial cell, denature ribosomes and suppress the required essential enzymes and proteins expression, especially for ATP production, which leads to cell disruption.[48]

In this study, co-treatments of PPE and AgNPs@PPE increases the anti-biofilm activity as even 1.0 mg/mL of

PPE showed anti-biofilm activity in the presence of 0.15 mg/mL and more concentrations of AgNPs@PPE. The interaction of ortho-phenolic hydroxyl functional groups of ellagic acid content of the peel extract with silver ions causes the esterification of the hydroxyl and carboxyl which is in accordance with the *p* track conjugation effect (flow of the electron density from a filled *p* or π orbital to an empty neighbor σ* orbital). As a result, the ortho-phenolic hydroxyl group loses the hydrogen easily, forming a steadier semi-quinone structure. Thus, ellagic acid causes H^+ radical formation that reduces the Ag^+ to AgNPs.[49] This is a probable mechanism of the synergetic effects of AgNPs@PPE and PPE co-treatment.

After 6, 12, 18, and 24 hrs of incubation, the decrease in biofilm formation rate was significant and inhibition percentages were higher. This could show a different impact of treatments which are parallel to different growth rates at different phases of growth followed by change in the gene expression profile.

Conclusion

PPE was used for the biosynthesis of AgNPs. This plant extract acts as reducing and stabilizing agent. The synthesized AgNPs@PPE was characterized by XRD, UV-vis, PL, and TEM. The characterization data showed AgNPs@PPE as fcc crystalline spherical nanoparticles with SPR free electron on its surface. The *P. aeruginosa* anti-biofilm formation activity was evaluated against the co-treatments of AgNPs@PPE and PPE. As a result, co-treatment of 1.0 mg/mL PPE and 0.15 mg/mL AgNPs@PPE significantly decreased the biofilm formation rate. Furthermore, no significant toxicity of AgNPs@PPE was shown against L929 cell line at 400 µg/mL concentration.

Compliance with ethical standards

This article does not contain any studies with human participants or animals performed by any of the authors.

Disclosure

The authors declare that they have no conflicts of interest in this work.

References

1. Bogino PC, Oliva Mde L, Sorroche FG, Giordano W. The role of bacterial biofilms and surface components in plant-bacterial associations. *Inter J Molecul Sci*. 2013;14:15838–15859.
2. Singh P, Pandit S, Garnæs J, et al. Green synthesis of gold and silver nanoparticles from Cannabis sativa (industrial hemp) and their capacity for biofilm inhibition. *Int J Nanomed*. 2018;13:3571–3591.
3. Allesen-Holm M, Barken KB, Yang L, et al. A characterization of DNA release in Pseudomonas aeruginosa cultures and biofilms. *Mol Microbiol*. 2006;59:1114–1128. doi:10.1111/mmi.2006.59.issue-4
4. Fu -Y-Y, Zhang L, Yang Y, et al. Synergistic antibacterial effect of ultrasound microbubbles combined with chitosan-modified polymyxin B-loaded liposomes on biofilm-producing Acinetobacter baumannii. *Int J Nanomed*. 2019;14:1805–1815. doi:10.2147/IJN.S186571
5. Alhariri M, Majrashi MA, Bahkali AH, et al. Efficacy of neutral and negatively charged liposome-loaded gentamicin on planktonic bacteria and biofilm communities. *Int J Nanomed*. 2017;12:6949–6961. doi:10.2147/IJN.S141709
6. Zhang X, Geng H, Gong L, et al. Modification of the surface of titanium with multifunctional chimeric peptides to prevent biofilm formation via inhibition of initial colonizers. *Int J Nanomed*. 2018;13:5361–5375. doi:10.2147/IJN.S170819
7. Costerton B. Microbial ecology comes of age and joins the general ecology community. *Proc Natl Acad Sci USA*. 2004;101:16983–16984. doi:10.1073/pnas.0407886101
8. Machado MC, Webster TJ. Decreased Pseudomonas aeruginosa biofilm formation on nanomodified endotracheal tubes: a dynamic lung model. *Int J Nanomed*. 2016;11:3825–3831. doi:10.2147/IJN.S108253
9. Nagaveni S, Rajeswari H, Oli AK, Patil SA, Chandrakanth RK. Widespread emergence of multidrug resistant Pseudomonas aeruginosa isolated from CSF samples. *Ind J Micro*. 2011;51(1):2–7. doi:10.1007/s12088-011-0062-0
10. Celik I, Temur A, Isik I. Hepatoprotective role and antioxidant capacity of pomegranate (Punica granatum) flowers infusion against trichloroacetic acid-exposed in rats. *Food Chem Toxicol*. 2009;47:145–149. doi:10.1016/j.fct.2008.10.020
11. Harue-Endo E, Ueda-Nakamura T, Nakamura CV, Dias Filho PB. Activity of spray-dried microparticles containing pomegranate peel extract against candida albicans. *Molecules*. 2012;17:10094–10107. doi:10.3390/molecules170910094
12. Ismail T, Sestili P, Akhtar S. Pomegranate peel and fruit extracts: a review of potential anti-inflammatory and anti-infective effects. *J Ethnopharmacol*. 2012;143(2):397–405. doi:10.1016/j.jep.2012.07.004
13. Meléndez PA, Capriles VA. Antibacterial properties of tropical plants from Puerto Rico. *Phytomed*. 2006;13(4):272–276. doi:10.1016/j.phymed.2004.11.009
14. Machado TB, Leal ICR, Amaral ACF, Santos KRN, Silva MG, Kuster RM. Antimicrobial ellagitannin of punica granatum fruits. *J Braz Chem Soc*. 2002;13:606–610. doi:10.1590/S0103-50532002000500010
15. Braga LC, Leite AAM, Xavier KGS, et al. Synergic interaction between pomegranate extract and antibiotics against Staphylococcus aureus. *Can J Microb*. 2005;51:541–547.
16. Dahham SS, Ali MN, Tabassum H. Studies on antibacterial and antifungal activity of pomegranate (Punica granatum L.). *Am Eurasian J Agric Environ Sci*. 2010;9(3):273–281.
17. Salunke GR, Ghosh S, Santosh Kumar RJ, et al. Rapid efficient synthesis and characterization of silver, gold, and bimetallic nanoparticles from the medicinal plant Plumbago zeylanica and their application in biofilm control. *Int J Nanomed*. 2014;9:2635–2653.
18. Liao S, Zhang Y, Pan X, et al. Antibacterial activity and mechanism of silver nanoparticles against multidrug-resistant Pseudomonas aeruginosa. *Int J Nanomed*. 2019;14:1469–1487. doi:10.2147/IJN.S191340
19. Iravani S, Korbekandi H, Mirmohammadi SV, Zolfaghari B. Synthesis of silver nanoparticles: chemical, physical and biological methods. *Res Pharm Sci*. 2014;9(6):385–406.
20. Zhang XF, Liu ZG, Shen W, Gurunathan S. Silver nanoparticles: synthesis, characterization, properties, applications, and therapeutic approaches. *Int J Mol Sci*. 2016;17:1534. doi:10.3390/ijms17091534

21. Długosz O, Banach M. Continuous production of silver nanoparticles and process control. *J Cluster Sci*. 2019;30:541–552. doi:10.1007/s10876-019-01505-y
22. Saravanan M, Arokiyaraj S, Lakshmi T, Pugazhendhi A. Synthesis of silver nanoparticles from Phenerochaete chrysosporium (MTCC-787) and their antibacterial activity against human pathogenic bacteria. *Microb Pathog*. 2018;117:68–72. doi:10.1016/j.micpath.2018.02.008
23. Pugazhendhi A, Prabakar D, Jacob JM, Karuppusamy I, Saratale RG. Synthesis and characterization of silver nanoparticles using Gelidium amansii and its antimicrobial property against various pathogenic bacteria. *Microb Pathog*. 2018;114:41–45. doi:10.1016/j.micpath.2017.11.013
24. Saravanan M, Barik SK, MubarakAli D, Prakash P, Pugazhendhi A. Synthesis of silver nanoparticles from Bacillus brevis (NCIM 2533) and their antibacterial activity against pathogenic bacteria. *Microb Pathog*. 2018;116:221–226. doi:10.1016/j.micpath.2018.01.038
25. Oves M, Aslam M, Rauf MA, et al. Antimicrobial and anticancer activities of silver nanoparticles synthesized from the root hair extract of Phoenix dactylifera. *Mater Sci Eng C Mater Biol Appl*. 2018;89:429–443. doi:10.1016/j.msec.2018.03.035
26. Pugazhendhi A, Edison TNJI, Karuppusamy I, Kathirvel B. Inorganic nanoparticles: a potential cancer therapy for human welfare. *Int J Pharm*. 2018;539(1–2):104–111. doi:10.1016/j.ijpharm.2018.01.034
27. Saratale RG, Karuppusamy I, Saratale GD, et al. A comprehensive review on green nanomaterials using biological systems: recent perception and their future applications. *Colloids Surf B Biointerfaces*. 2018;170:20–35. doi:10.1016/j.colsurfb.2018.05.045
28. Shankar PD, Shobana S, Karuppusamy I, et al. A review on the biosynthesis of metallic nanoparticles (gold and silver) using bio-components of microalgae: formation mechanism and applications. *Enzyme Microb Technol*. 2016;95:28–44. doi:10.1016/j.enzmictec.2016.10.015
29. Ramkumar VS, Pugazhendhi A, Gopalakrishnan K, et al. Biofabrication and characterization of silver nanoparticles using aqueous extract of seaweedEnteromorpha compressa and its biomedical properties. *Biotechnol Rep (Amst)*. 2017;14:1–7. doi:10.1016/j.btre.2017.02.001
30. Saratale GD, Saratale RG, Benelli G, et al. Anti-diabetic potential of silver nanoparticles synthesized with Argyreia nervosa leaf extract high synergistic antibacterial activity with standard antibiotics against foodborne bacteria. *J Cluster Sci*. 2017;28:1709–1727. doi:10.1007/s10876-017-1179-z
31. Fernandes RA, Berretta AA, Torres EC, et al. Antimicrobial potential and cytotoxicity of silver nanoparticles phytosynthesized by pomegranate peel extract. *Antibiotics (Basel)*. 2018;7(3):51. doi:10.3390/antibiotics7030077
32. Nasiriboroumand M, Montazer M, Barani H. Preparation and characterization of biocompatible silver nanoparticles using pomegranate peel extract. *J Photochem Photobiol B*. 2018;179:98–104. doi:10.1016/j.jphotobiol.2018.01.006
33. Sahraei R, Farmany A, Mortazavi SS. A nanosilver-based spectrophotometry method for sensitive determination of tartrazine in food samples. *Food Chem*. 2013;138:1239–1242. doi:10.1016/j.foodchem.2012.11.029
34. O'toole GA. Microtiter dish biofilm formation assay. *JoVE*. 2011;47. doi:10.3791/2437
35. Nyenje ME, Green E, Ndip RN. Biofilm formation and adherence characteristics of listeria ivanovii strains isolated from ready-to-eat foods in Alice, South Africa. *Sci World J*. 2012;873909. doi:10.1100/2012/873909
36. Méndez-Vilas A, Ed. *Communicating Current Research and Educational Topics and Trends in Applied Microbiology*. Badajoz: Formatex; 2007. .
37. Namasivayam SKR, Preethi M, Bharani RS, Robin G, Latha B. Biofilm inhibitory effect of silver nanoparticles coated catheter against Staphylococcus aureus and evaluation of its synergistic effects with antibiotics. *Int J Pharm Sci Rev Res*. 2012;3(2):259–265.
38. Suvith VS, Philip D. Catalytic degradation of methylene blue using biosynthesized gold and silver nanoparticles. *Spectrochim Acta A Mol Biomol Spectrosc*. 2014;118:526–532. doi:10.1016/j.saa.2013.09.016
39. Kumar V, Yadav SK. Plant mediated synthesis of silver and gold nanoparticles and their applications. *J Chem Technol Biotechnol*. 2009;84:151–157. doi:10.1002/jctb.v84:2
40. Anandalakshmi K, Venugobal J, Ramasamy V. Characterization of silver nanoparticles by green synthesis method using Pedalium murex leaf extract and their antibacterialactivity. *Appl Nanosci*. 2016;6:399–408. doi:10.1007/s13204-015-0449-z
41. Haslam E. Natural polyphenols (vegetable tannins) as drugs: possible modes of action. *J Nat Prod*. 1996;59:205–215.
42. Vasconcelos LC, Sampaio MC, Sampaio FC, Higino JS. Use of Punica granatum as an antifungal agent against candidosis associated with denture stomatitis. *Mycoses*. 2003;46:192–196. doi:10.1046/j.1439-0507.2003.00884.x
43. Stern JL, Hagerman AE, Steinberg PD, Mason PK. Phlorotannin-protein interactions. *J Chem Ecol*. 1996;22:1887–1899. doi:10.1007/BF02028510
44. Jefferson KK. What drives bacteria to produce a biofilm? *FEMS Microb Lett*. 2004;236:163–173. doi:10.1111/j.1574-6968.2004.tb09643.x
45. Li WR, Xie XB, Shi QS, Zeng HY, Ou-Yang YS, Chen YB. Antibacterial activity and mechanism of silver nanoparticles on Escherichia coli. *Appl Microb Biotech*. 2010;85(4):1115–1122. doi:10.1007/s00253-009-2159-5
46. Silva T, Pokhrel LR, Dubey B, Tolaymat TM, Maier KJ, Liu X. Particle size, surface charge and concentration dependent ecotoxicity of three organo-coated silver nanoparticles: comparison between general linear model-predicted and observed toxicity. *Sci Total Environ*. 2014;468–469:968–976.
47. Park HJ, Park S, Roh J, et al. Biofilm-inactivating activity of silver nanoparticles: a comparison with silver ions. *J Ind Eng Chem*. 2013;19:614–619. doi:10.1016/j.jiec.2012.09.013
48. Méndez-Vilas A, Ed. Microbial pathogens and strategies for combating them. *Sci Technol Educ*. Badajoz: Formatex; 2013.
49. Ahmad N, Sharma S, Rai R. Rapid green synthesis of silver and gold nanoparticles using peels of Punica granatum. *Adv Mater Lett*. 2012;3(5):376–380.